Optimizing Transcutaneous Carbon Dioxide Measurement Sites on Humans

Nilgun Duman*, Alper Y. Ozbey*, Isil Isiksalan¹, and Ulkuhan Guler¹

Abstract—This study explores the body sites for measuring transcutaneous carbon dioxide (CO₂) noninvasively using a miniaturized monitor that employs a technique known as timedomain dual lifetime referencing. Accurate measurement of CO2 levels is crucial for patients with respiratory distress who need monitoring in both clinical and home care settings. We tested this novel monitor by calculating ratio values of luminescence light, indicative of CO₂ levels, at five different body locations: cheek, forearm, forehead, wrist, and fingertip, on four subjects. We also conducted a repeatability analysis: we tested the sensor on one subject at the fingertip each day for three consecutive days. Our findings show that while all tested sites presented reliable data, the forehead and cheek yielded faster settling times, and the forearm, forehead, and wrist produced less variation in readings. The results highlight the significance of choosing effective sites for accurate transcutaneous CO₂ monitoring.

Index Terms—Transcutaneous Carbon Dioxide Sensing, Noninvasive Blood Gas Measurement, Physiological Monitoring, Wearable Devices, Luminescence Sensing.

I. INTRODUCTION

Impaired exchange of blood gases continues to pose significant challenges in healthcare, with conditions ranging from community-acquired pneumonia to diabetic ketoacidosis, contributing to a high mortality burden among neonates and children [1], [2]. Both diseases obstruct the lungs, causing excessive levels of carbon dioxide (CO₂) in the blood as the lungs fail to remove CO₂, eventually leading a patient into a state of hypercapnia [3]. These fatalities can be attributed to the unavailability of tools to monitor the progression of the illness severity through continuous blood CO₂ level measurements. Consequently, the conditions in neonates and children require technology that continuously and noninvasively monitors the patient's blood gas levels to allow healthcare professionals to intervene and efficiently provide necessary treatment [4].

Monitoring CO₂ levels in the human body is crucial for assessing respiratory function and identifying issues with regulating metabolic pathways [5]. Contemporary options compromise of invasive techniques like arterial blood gas (ABG) analysis, capillary blood gas (CBG), and venous blood gas (VBG) [6]. Among them, ABG, measuring the partial pressure of carbon dioxide (PaCO₂) in the arteries, is the most reliable method available; in other words, it is the golden standard for assessing CO₂ [7]. Despite its accuracy, ABG analysis

*These authors contributed equally to this work. ¹Authors are with the Department of Electrical and Computer Engineering, Worcester Polytechnic Institute, Worcester, MA, USA (e-mail: {uguler}@wpi.edu).

This material is based upon work in part supported by the National Science Foundation (NSF) under Grant ECCS-2143898 and National Institute of Health (NIH) under Grant 1R21EB036329-01. Corresponding author: Ulkuhan Guler.

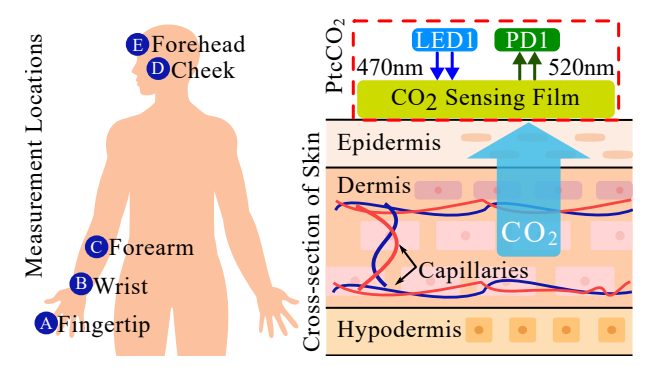


Fig. 1. Transcutaneous carbon dioxide measurement sites on humans.

contains its own constraints: it creates an uncomfortable and painful environment [8], changes in respiratory status being identified are contingent on new blood samples every time [7], entails substantial cost, restricted availability, requires a physician to place a catheter to the artery [9], dangerous complications, infectious risk, and significant blood loss [10].

CO₂ has been recognized to spread throughout the capillaries and epidermis, forming a measurable partial pressure of CO₂ on the surface of the skin, referred to as partial pressure of transcutaneous carbon dioxide (PtcCO₂) [11]. Due to the established correlation between PaCO₂ and PtcCO₂ [12], transcutaneous monitoring offers a viable alternative to invasive methods [4]. This noninvasive approach enables continuous, remote monitoring of CO₂ levels, significantly reducing patient discomfort by eliminating the need for frequent arterial punctures and making it particularly suitable for those requiring gentle care.

Traditionally, heated electrochemical sensors are placed on the skin to measure PtcCO2 levels. However, heating the sensor will lead to excessive power consumption [13]. Alternatively, CO₂-sensitive luminescent materials provide an option that avoids heating. These materials contain luminophores, which, when illuminated, transition to an excited state. Upon returning to their ground state, they emit light, a process known as luminescence [14]. Luminescent sensors are particularly advantageous for wearable applications due to their small size, rapid response, and high sensitivity [15], whereas wet electrode-based sensors cannot be transferred into a smaller footprint, limiting their extensive use outside clinical settings [16]. Recent advancements in luminescencebased CO₂ sensing have introduced the time-domain dual lifetime referencing (t-DLR) technique. This method improves the accuracy of PtcCO₂ measurements by compensating for intensity fluctuations and the short lifetimes in the luminescence

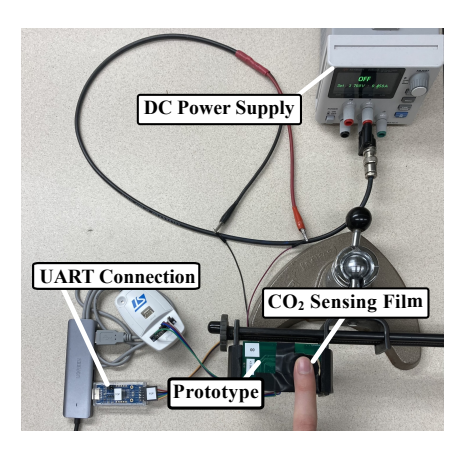


Fig. 2. Measurement setup for human subject tests.

curve [15].

The t-DLR technique employs two types of luminophores within the sensor film: CO₂-sensitive and reference luminophores. While CO₂-sensitive luminophores vary their output based on CO₂ levels, the reference luminophores provide consistent data. By establishing mathematical expressions for both types of luminophores when illumination is ON/OFF, a ratio (A_{ON}/A_{OFF}) is formed. A_{ON} accounts for the luminescence of both luminophores, whereas A_{OFF} is based solely on the reference luminophore. In this case, the term that represents various external factors is canceled, revealing a technique in which only necessary luminescence information is captured without the use of complicated technology that disrupts the purpose of a miniature, wearable device [15], [17], [18].

This study aims to evaluate the performance of a t-DLR-based PtcCO₂ sensor on its performance across multiple body sites to determine the optimal locations for accurate and reliable CO₂ monitoring and its repeatability. By comparing the settlement time and normalized CO₂ ratio values across these sites, we seek to identify specific body areas where the transcutaneous method can provide data with the highest fidelity. The subsequent sections of this manuscript are organized as follows. Section II briefly describes the previous prototyping work to set the background of the device presented in this paper. Section III explains the measurement protocol and data collection methods. Sections IV and V demonstrate the results and discuss our findings, respectively, followed by the concluding remarks in Section VI.

II. PREVIOUS WORK

A wearable prototype capable of measuring $PtcCO_2$ using a miniaturized, custom-designed printed circuit board is presented in [19]. Initially created for transcutaneous oxygen $(PtcO_2)$ monitoring [20], [21], this device has been adapted to measure $PtcCO_2$ by incorporating a luminescent sensing film sensitive to CO_2 levels. The design modifications included replacing the light-emitting diode (LED) and photodetector (PD) to accommodate the new CO_2 -sensitive film. The prototype employs the t-DLR technique to improve the accuracy of CO_2 measurements [17]. The firmware has been developed

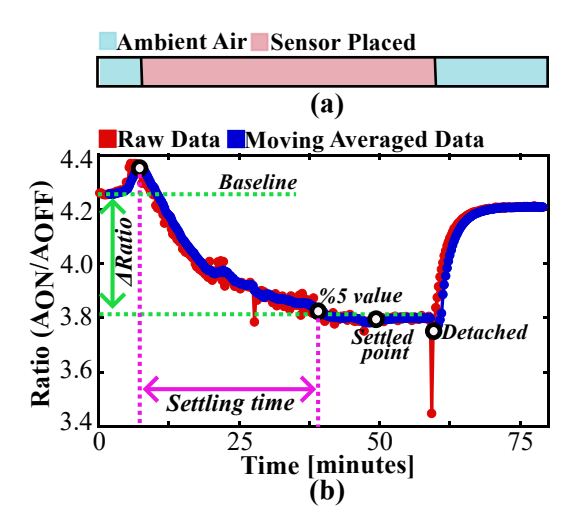


Fig. 3. (a) Measurement protocol; (b) Forearm measurement from Subject 2.

to calculate luminescence ratio values onboard, providing updated measurements every 15 seconds. Preliminary tests conducted in gas chambers and with human subjects have demonstrated the prototype's potential, effectively tracking changes in CO₂ levels with high resolution [19].

A. Instrumentation

The prototype, illustrated in Fig. 2, comprises four primary blocks: a power management unit (PMU), a sensor head, an analog front end (AFE), and a microcontroller unit (MCU). It is powered by an external DC power supply providing voltage and current levels of 3.1 V and 250 mA, respectively. On top of the sensor head is a luminescent CO₂-sensitive film (SP-CD1-D5-rMy-US by Pre-Sens Precision Sensing). The emission spectra of the film and luminescence curves from reference and CO₂-sensitive luminophores are explained in detail in [15]. The sensor head includes a blue LED (LXZ1 PR0 by Lumileds) with a peak emission at 470 nm and a PD (SD019-141-411-G by Advanced Photonix) sensitive to green light with a peak around 520 nm.

The AFE, model ADPD4101 by Analog Devices Inc., performs several operations, including driving the LED, processing the optical response of the PD into an analog signal, and digitizing this signal for storage in its first-in-first-out (FIFO) memory buffer. The MCU, model STM32WB35CC by STMicroelectronics, is configured to manage the AFE settings, perform t-DLR calculations, and transmit the calculated lifetime and ratio data to a PC via a Universal Asynchronous Receiver-Transmitter (UART) interface with a data sampling rate of every 15 seconds using PuTTY. Further details about the original system design can be found in previous work [20], and the modifications made for PtcCO₂ measurements and corresponding firmware updates are detailed in [19]. The entire test setup is depicted in Fig. 2.

III. PROTOCOL AND DATA COLLECTION

A. Measurement Protocol

A consistent measurement protocol, illustrated in Fig. 3a, was followed for each test. Before placing the body part that is being measured on the sensor, the sensor was turned on for 5 minutes to collect data measuring ambient air. This initial measurement was crucial as it established a baseline ratio for the experiment. After 5 minutes, the body part that was being measured was placed on the sensor for 55 minutes. Next, another measurement is taken for 20 minutes in ambient air to examine the time it takes for the sensor to return to baseline. The same protocol is followed for both repeatability and location analysis.

B. Data Collection and Post-processing

We utilized a Python script to process the data received via a UART interface, which was saved in a PuTTY log. At the end of each experiment, we post-processed the ratio data to remove outliers and applied a moving average with a window size of 8, corresponding to a 2-minute window. The raw and averaged data for the forearm measurement taken from Subject 2 are shown as an example in Fig. 3b.

For the first five minutes of the experiment, as seen in Fig. 3a, the sensor was in ambient air. We applied linear regression to the baseline ratio points to obtain the baseline ratio value for reference and again to the settled ratio points to derive the settled ratio value. The difference between the baseline and settled ratios, referred to as $\Delta Ratio$, is illustrated in Fig. 3b. Since the sensing film's baseline changes due to factors such as photobleaching and part-to-part variation, we also defined a normalized $\Delta Ratio$, which is the delta ratio divided by the baseline ratio. This normalized value allows for a more fair comparison of results with each other. After calibration, this normalized $\Delta Ratio$ value from each measurement can be used to interpret PtcCO2 levels. Afterward, we calculated the settling time of the ratio values, also depicted in Fig. 3b. The settling time was identified using two points: first, the time when the sensor is attached to the measurement site, and second, the point at which the ratio drops to 95% of the range from the baseline ratio value in ambient air to the stabilized ratio value on the human subject. The time between these two points is referred to as the settling time.

IV. RESULTS AND FINDINGS

A. Repeatability tests

The repetitive collection of fingertip values was recorded on test Subject 2 routinely for three days. With one fingertip measurement from the subject a day, we acquired a total of three fingertip measurements under the strict uniform procedure. The repeatability tests followed the same process stated in Section III. Factors such as attaining sufficient sleep (at least 7 hours), waking up at a set time, and having a similar diet throughout the testing days were a part of the process to maximize the potential of our findings. Table I shows the settlement time, settled ratio, $\Delta Ratio$, and normalized

TABLE I REPEATABILITY ANALYSIS

Day	Settlement Time (min)	Settled Ratio	Δ Ratio	Normalized $\Delta Ratio$
1	42.25 min	3.50	0.07	2.03%
2	40.25 min	3.50	0.06	1.78%
3	36.75 min	3.46	0.08	2.32%

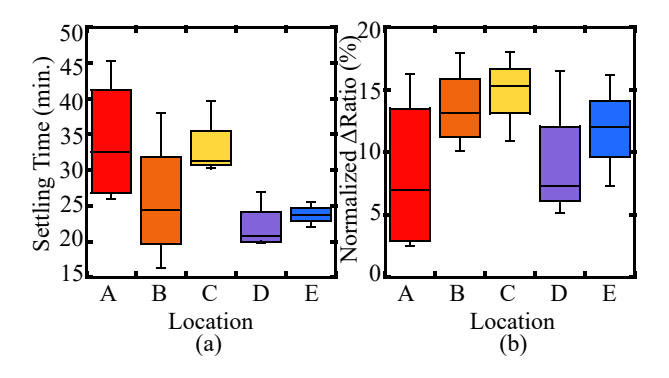


Fig. 4. Distribution of experimental data among locations for (a) settling time and (b) normalized $\Delta Ratio$ (locations are denoted as: A - fingertip, B - wrist, C - forearm, D - cheek, and E - forehead).

 $\Delta Ratio$ for all repetition trials at the end of three days. A great settlement time consistency was seen within all of the measurements, with the average settlement time being 39.75 minutes and a variation of 5.5 minutes between the repeatability measurements. A similar consistency in $\Delta Ratio$ was observed, with a slight variation of 0.54%. These measurements are presented in Fig. 5b.

B. Location tests

The luminescence ratio values of various body locations, including fingertip, forearm, wrist, forehead, and cheek, were measured on four different test subjects. The locations can be seen in Fig. 1, and their distribution of settling times and luminescence $\Delta Ratio$ values are depicted in Table II and visualized in Figs. 4a and 4b, respectively. The settling times and normalized $\Delta Ratio$ values varied across the test subjects; however, the measurement outputs of the forehead had considerably less variation in settlement times, between 22-25.5 min, while the forearm had the least variation in normalized $\Delta Ratio$ values, between 10.93%-18.06%, than the rest. The cheek was the quickest to reach its settling time, with an average of 22.06 min. On the other hand, the wrist had the most variation of settlement times between 16.25-38 min, and the fingertip had the largest variation of $\Delta Ratio$ values between 2.49%-16.28%.

V. DISCUSSION

Factors such as settlement time and normalized $\Delta Ratio$ were involved in determining the most feasible body locations for PtcCO₂ monitoring. Fig. 5 demonstrates that our system successfully collected the data samples from each body location. Fig. 5a shows measurements from one subject across all identified measurement sites. Before placing the sensor on the

'	Subject 1		Subject 2		Subject 3		Subject 4	
Body Site	Settling Time	$\Delta Ratio$ / normalized $\Delta Ratio$	Settling Time	$\Delta Ratio$ / normalized $\Delta Ratio$	Settling Time	$\Delta Ratio$ / normalized $\Delta Ratio$	Settling Time	$\Delta Ratio$ / normalized $\Delta Ratio$
Fingertip	26 min	0.5 / 10.73%	37.25 min	0.09 / 2.49%	27.75 min	0.75 / 16.28%	45.25 min*	0.12 / 3.23%
Wrist	25.75 min	0.43 / 10.11%	38 min	0.63 / 13.89%	16.25 min	0.85 / 17.93%	23 min	0.52 / 12.4%
Forearm	31.25 min	0.72 / 15.31%	39.75 min	0.47 / 10.93%	30.25 min	0.81 / 18.06%	NA	NA
Forehead	NA	NA	23.75 min	0.29 / 7.32%	25.5 min	0.7 / 16.2%	22 min	0.49 / 12.0%
Cheek	27 min	0.29 / 7.04%	20.25 min	0.2 / 5.11%	21.25 min	0.3 / 7.59%	19.75 min	0.71 / 16.53%

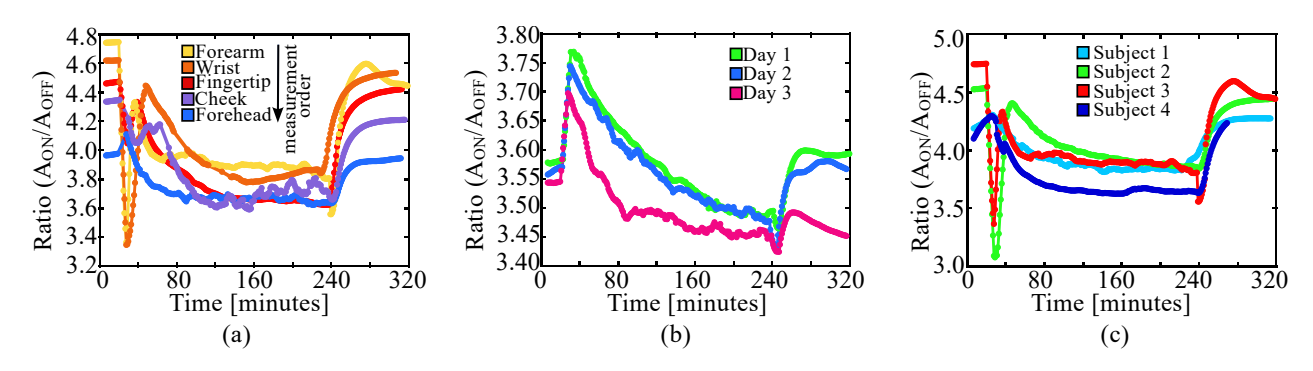


Fig. 5. (a) Subject 3 measurements for all locations, (b) All subject 2 fingertip measurements (repeatability tests), and (c) Wrist measurements for all 4 subjects are shown.

body location, the sensing film was left in ambient air for 5 minutes. As depicted, while we conducted the experiments, we used the same film for Subject 3. During the measurements, the sensing film experienced photobleaching, causing the film's baseline value to change. Photobleaching occurs when luminophore molecules permanently lose their ability to luminesce after prolonged light exposure [22], a major constraint in our data collection process. This deterioration of the CO₂ sensing film limits its usability to 10-12 measurements of 80-minute intervals. Moreover, we want to emphasize that the photobleaching process necessitates calibration algorithms to minimize photobleaching-rooted errors, which is considered as a future work in this project.

Because of the baseline shift due to photobleaching, to analyze and elucidate the results, we focused on the normalized $\Delta Ratio$ instead of the $\Delta Ratio$ for a fair comparison and interpretation of the findings. The baseline change is also evident in Fig. 5b, which shows repeatability analysis. Additionally, the repeatability tests provided that the fingertip was an optimal location for consistent data outputs; however, when compared to the measurements from other sites, it wasn't the most favorable in terms of settling time.

All the data collected from the four subjects are presented in Table II, and the distribution of this data is depicted in Fig. 4. From this data, it can be observed that the cheek and forehead demonstrate faster settlement times, and the forearm and wrist provide more consistent variations throughout the normalized $\Delta Ratio$ values. These variations among the four subjects are expected, as each subject varies in body weight and fat and muscle mass distribution, which results in distinct

diffusion rates of CO_2 to various body locations [15]. These differences, coupled with the photobleaching of the sensing film, account for the variations in the $\Delta Ratio$. This is also exemplified through Fig. 5c, which showcases measurements taken from the wrist for all 4 subjects, yet each subject has different resulting values due to such factors.

In addition to these locations, the forearm also showed results with relatively slower settlement times and measurement data values that were less noisy, making it easier to identify the 5% and settled points, as shown in Fig. 3b. Although the forearm is generally regarded as a body part with thicker skin [23] that could affect the accuracy of measurements, the position in which subjects conducted their forearm measurements left little to no room for movement, mitigating the influence of wired connections that impact the variation of values and present a slower settling time. The opposite is true for cheek measurements; due to its softness and unsteady nature, involuntary movement caused noisy settling data that disrupted the structure of settling time analysis.

For further use, the post-processing algorithm should be enhanced to better interpret the settled ratio line in noisy measurement locations. Improving the algorithm's ability to handle variability in noisy signals will be crucial for obtaining more accurate and reliable results. By implementing a technique that could increase the efficiency and validity of measurement outputs, a broader variety of measurement locations and their results would be viable.

VI. CONCLUSION

This study successfully evaluated the effectiveness of a novel miniaturized PtcCO₂ monitor using the t-DLR technique across various body sites. The findings demonstrate that the forehead is a promising site for PtcCO₂ monitoring due to its faster settling times and more consistent measurement outputs. Additionally, the placement of the forearm allowed for the removal of several factors that affected the results, providing more identifiable and consistent data. In contrast, the cheek's susceptibility to those same variables presented challenges such as noisier data. Future research should focus on expanding the study to include a larger population, and implementing a stricter measurement protocol to record interpersonal parameters could provide further insights into optimizing PtcCO2 monitoring for broader clinical applications. Overall, this research advances the development of noninvasive monitoring solutions, offering potential improvements in patient care and the management of respiratory conditions.

ACKNOWLEDGMENT

We would like to express our sincere appreciation to Tuna Berk Tufan, Ph.D. Candidate, for his contributing ideas and assistance throughout this research

REFERENCES

- S. Sazawal and R. E. Black, "Effect of pneumonia case management on mortality in neonates, infants, and preschool children: a meta-analysis of community-based trials," *The Lancet infectious diseases*, vol. 3, no. 9, pp. 547–556, 2003.
- [2] R. A. Shimelash et al., "Incidence and predictors of mortality in children with diabetic ketoacidosis in the comprehensive specialized referral hospitals of west amhara region, northwest ethiopia: a retrospective follow-up study," Frontiers in Clinical Diabetes and Healthcare, vol. 4, 2023.
- [3] D. Rawat et al., "Hypercapnea," in StatPearls [Internet]. StatPearls Publishing, 2023.
- [4] D. Sankaran et al., "Non-invasive carbon dioxide monitoring in neonates: methods, benefits, and pitfalls," *Journal of Perinatology*, vol. 41, no. 11, pp. 2580–2589, 2021.
- [5] K. Perrin et al., "Assessing paco2 in acute respiratory disease: accuracy of a transcutaneous carbon dioxide device," *Internal medicine journal*, vol. 41, no. 8, pp. 630–633, 2011.
- [6] K. P. Sullivan et al., "Transcutaneous carbon dioxide pattern and trend over time in preterm infants," *Pediatric Research*, vol. 90, no. 4, pp. 840–846, 2021.

- [7] J. D. Tobias, "Transcutaneous carbon dioxide monitoring in infants and children," *Pediatric Anesthesia*, vol. 19, no. 5, pp. 434–444, 2009.
- [8] A. Goenka et al., "Neonatal blood gas sampling methods," South African Journal of Child Health, vol. 6, no. 1, pp. 3–9, 2012.
- [9] I. Costanzo et al., "Respiratory monitoring: Current state of the art and future roads," *IEEE Reviews in Biomedical Engineering*, vol. 15, pp. 103–121, 2020.
- [10] J. C. Das et al., "Monitoring of oxygen in neonate: An important issue," Journal of Chittagong Medical College Teachers' Association, vol. 21, no. 2, pp. 30–34, 2010.
- [11] W. Van Weteringen *et al.*, "Validation of a new transcutaneous tcpo2/tcpco2 sensor with an optical oxygen measurement in preterm neonates," *Neonatology*, vol. 117, no. 5, pp. 628–636, 2021.
- [12] M. Dicembrino *et al.*, "End-tidal co2 and transcutaneous co2: Are we ready to replace arterial co2 in awake children?" *Pediatric Pulmonology*, vol. 56, no. 2, pp. 486–494, 2021.
- [13] I. Costanzo et al., "A noninvasive miniaturized transcutaneous oxygen monitor," *IEEE Transactions on Biomedical Circuits and Systems*, vol. 15, no. 3, pp. 474–485, 2021.
- [14] J. R. Lakowicz, Principles of fluorescence spectroscopy. Springer, Sept. 2006. Boston, MA.
- [15] T. B. Tufan and U. Guler, "A Transcutaneous Carbon Dioxide Monitor Based on Time-Domain Dual Lifetime Referencing," *IEEE Transactions* on Biomedical Circuits and Systems, pp. 1–12, 2023.
- [16] A. Leonardi et al., "Optimizing transcutaneous oxygen measurement sites on humans," in 2023 45th Annual International Conference of the IEEE Engineering in Medicine & Biology Society (EMBC), 2023, pp. 1–4.
- [17] T. B. Tufan and U. Guler, "A transcutaneous carbon dioxide monitor based on time-domain dual lifetime referencing," *IEEE Transactions on Biomedical Circuits and Systems*, vol. 17, no. 4, pp. 795–807, 2023.
- [18] I. Klimant et al., "Dual lifetime referencing (dlr)—a new scheme for converting fluorescence intensity into a frequency-domain or timedomain information," in New trends in fluorescence spectroscopy: applications to chemical and life sciences. Springer, 2001, pp. 257–274.
- [19] K. Golemi et al., "A wearable prototype measuring ptcco2 and spo2," in 2024 IEEE Biomedical Circuits and Systems Conference (BioCAS). IEEE, 2024, pp. 1–5.
- [20] B. Kahraman et al., "A miniaturized prototype for continuous noninvasive transcutaneous oxygen monitoring," in 2022 IEEE Biomedical Circuits and Systems Conference (BioCAS). IEEE, 2022, pp. 486–490.
- [21] V. Vakhter et al., "A prototype wearable device for noninvasive monitoring of transcutaneous oxygen," IEEE Transactions on Biomedical Circuits and Systems, vol. 17, no. 2, pp. 323–335, 2023.
- [22] A. B. Houtsmuller, Fluorescence Recovery after Photobleaching: Application to Nuclear Proteins. Berlin, Heidelberg. Springer Berlin Heidelberg, 2005, pp. 177–199.
- [23] T. Van Mulder et al., "High frequency ultrasound to assess skin thickness in healthy adults," Vaccine, vol. 35, no. 14, pp. 1810–1815, 2017.